



## Study on the relationship between the oxidation degree of GO and the adsorption capacity for $Pb^{2+}$

Liu Xiao\*<sup>1,2,3</sup>, Zhou Zihang<sup>1</sup>, Lisi Qi<sup>1</sup> & Liu Yan<sup>1</sup>

<sup>1</sup>College of Materials Science and Engineering, North Minzu University, Yinchuan 750021, China

<sup>1</sup>Collaborative Innovation Center for High Value Utilization of Industrial By-products, Yinchuan 750021, China

<sup>3</sup>International Scientific and Technological Cooperation Base of Industrial Waste Recycling and Advanced Materials, Yinchuan 750021, China

E-mail: plzlx@163.com

Received 19 September 2019; accepted 15 October 2020

In this study, four kinds of graphite oxide (GO) with different oxidation degree have been prepared by a modified Hummers method, by changing the amount of oxidation agent  $KMnO_4$ . To investigate the relationship between the oxidation degree of GO and the adsorption capacity for heavy metal ions,  $Pb^{2+}$  solution has been selected as a model waste water. The effects of initial  $Pb^{2+}$  concentration, solution  $pH$  and contact time on the adsorption capacity of series GO have been studied. It is found that the adsorption capacity does not always increase with the increasing of oxidation degree. The adsorption process of series GO for  $Pb^{2+}$  are well described by the Langmuir isotherm model, which reveals that the adsorption process is homogeneous monolayer coverage

**Keywords:** Adsorption, Graphite oxide, Oxidation degree,  $Pb^{2+}$

Heavy metals can be removed from aqueous media using various conventional methods such as chemical precipitation, solvent extraction, membrane filtration, ion exchange, electrochemical removal, coagulation etc<sup>1</sup>. However, adsorption is a cost-effective technology for the removal of heavy metals from the environment among all the methods, due to its low cost, efficiency and availability of a wide range of adsorbents, adsorption has received a significant attention<sup>2</sup>. Here-in, adsorbent plays a main role in the process of adsorption. Up to now, numerous adsorbents of different nature<sup>1</sup> (such as activated carbons, zeolites, clay minerals, industrial solid waste, and biomaterials) have been employed in initial or modified forms for removing noxious heavy metals ions from wastewater effluents.

Graphite oxide (GO) is one of the most easily-available derivatives of graphene, which consisting of various functional groups such as hydroxyl, carboxyl, and epoxy groups. Compared to the traditional adsorbents, GO is regarded as the most promising adsorbent to adsorb various heavy metal ions, due to its super large surface area and abundant adsorption sites (hydroxyl, carbonyl, carboxyl, epoxy) and  $\pi$ -electron system<sup>3-7</sup>. Generally speaking, the adsorption mechanisms of heavy metals onto GO may contain electrostatic attraction and surface complexation

between the heavy metal ions and the functional groups on the surface of GO composite. In some literatures<sup>8,9</sup>, electrostatic attraction has been proved as the controlling mechanism due to the strong attraction between the positively charged metal ions and the negative functional groups on the surface of the GO. However, surface complexation becomes the dominant mechanism controlling the removal of the heavy metal ions in some other instances. Liu *et al.*<sup>10</sup> studied the mechanism of Cu(II) adsorption using DCTA-MGO composite and observed that Cu(II) ions interacted directly with the carboxyl, hydroxyl, and amino groups to form surface complexes. Zare-Dorabei *et al.*<sup>11</sup> studied the adsorption of Pb(II), Cd(II), Ni(II) and Cu(II) using DPA-modified GO, with the surface complexation being the dominant mechanism. Tadjarodi *et al.*<sup>12</sup> used modified GO to remove Hg(II) and proved that the adsorption process contained surface complexation and electrostatic attraction. Whether it is electrostatic adsorption or surface complexation, the adsorption capacity would increase with the increasing of functional groups (carboxyl, hydroxyl, epoxy) on the surface of GO, theoretically.

In actually, the main mechanism would be determined strongly by the solution  $pH$ , metal speciation and the functional groups of the adsorbent,

and the adsorption process is a complex process<sup>13</sup>. In addition to electrostatic attraction and surface complexation, the aromatic matrixes in GO can provide a large number of delocalized  $\pi$ -electron to bind heavy metals through the Lewis acid-base interaction<sup>14,15</sup>. It means that the relative proportion of the oxygen-containing functional groups and aromatic groups within GO would affect the adsorption capacity for heavy metal ions, instead of the amount of oxygen-containing functional groups only. The oxygen-containing functional groups on GO can not only enhance its hydrophilicity, but also destroy  $sp^2$ -hybridized structure, resulting in weaker Lewis acid-base interactions with heavy metal ions<sup>16</sup>. Therefore, it is very necessary to study the relationship between the adsorption capacity and oxidation degree of GO.

In this study, we prepared four kinds of GO with a modified Hummers' method, by changing the amount of oxidation agent  $KMnO_4$ . The chemical structure of series GO were investigated by different characterizations. To study the effect of oxidation of GO on the adsorption capacity,  $Pb^{2+}$  solution was selected as model waste water. The effects of initial  $Pb^{2+}$  concentration, solution pH and contact time on the adsorption capacity of series GO were studied. Simultaneously, the adsorption isotherms were also investigated in details.

## Experimental Section

### Materials

Graphite powder was purchased from China National Pharmaceutical Group Corporation. Sulfuric acid ( $H_2SO_4$ ) and potassium permanganate ( $KMnO_4$ ) were obtained from Guangzhou Chemical Reagent Factory (China). All other chemicals used in the experiments were chemical grade and purchased from China National Pharmaceutical Group Corporation.

### Preparation of graphite oxide with different oxidation degree

GO was prepared by the Hummers method<sup>5</sup> with some modifications. Firstly, 50 mL of concentrated  $H_2SO_4$  and 1 g of  $NaNO_3$  was added into a 250 mL flask consecutively, and then the flask was cooled to  $0^\circ C$  in an ice bath. After this, 2g of natural graphite was added into the flask with stirring. To obtain a series of GO with different oxidation degree, different quality of solid  $KMnO_4$  (3g, 6g, 8g, 12g) was gradually added. The mixture was kept below  $20^\circ C$  and stirred for 2 h. Next the temperature was increased to  $35^\circ C$  and stirred continually for half an hour. 90 mL of distilled water was then added to the mixture and the temperature of the reaction

system increased to  $90^\circ C$ . After the mixture stirred for 0.5 h at  $90^\circ C$ , 30%  $H_2O_2$  was added until the colour of mixture changed to brilliant yellow and there was no gas being produced. The mixture was filtered and washed three times with 5% aqueous HCl to remove metal ions and then washed with distilled water to remove the acid. At last, the series GO with different oxidation degree were obtained after the filter cake was dried in air, named as GO-1, GO-2, GO-3 and GO-4, respectively. The detailed preparation conditions are listed in Table 1.

### Characterization

The chemical structures of samples were obtained in transmission mode on a Fourier-transform infrared spectrophotometer (FT-IR, American Nicolet Corp. Model 170-SX) using the KBr pellet technique; the crystal structure of samples were examined by the X-ray diffraction (XRD, Rigaku D/MAX-2400 X-ray diffractometer with Ni-filtered Cu  $K\alpha$  radiation); The morphologies of the samples were further investigated by transmission electron microscopy (TEM, FEI Tecnai G20) and scanning electron microscopy (SEM, Zeiss, Sigma500, Germany); The elemental composition of samples were examined by energy dispersive spectrometer (EDS, Zeiss, Sigma500, Germany); the zeta-potential of the samples were investigated by laser particle size analyzer (Malvern, Nano-ZS90, England).

### Adsorption experiment

Herein, the four kinds of GO (GO-1, GO-2, GO-3 and GO-4) were used to adsorb  $Pb^{2+}$  solution which was prepared from  $Pb(NO_2)_2$ . Necessary qualities of GO were put into  $Pb^{2+}$  solution, then the adsorption reaction was carried out in a shaking-table with rotational speed at 120 rpm for a certain time. After reaction completed, the residual concentration of  $Pb^{2+}$  was detected by UV-vis spectrophotometer at 580 nm using xylenol orange. The adsorption capacity and removal efficiency were calculated using the following equations:

$$Q = \frac{(C_0 - C_t) \times V}{M}$$

$$R(\%) = \frac{C_0 - C_t}{C_t} \times 100$$

Table 1 — The different amount of oxidant used for series GO

Samples	GO-1	GO-2	GO-3	GO-4
Graphite(g)	2	2	2	2
$KMnO_4$ (g)	3	6	8	12

where  $Q$  (mg/g) is the amount of Pb(II) adsorbed per unit amount of adsorbent,  $R$  (%) is the removal efficiency,  $C_0$  and  $C_t$  (mg/L) are the initial and instantaneous Pb(II) concentrations, respectively,  $V$  (L) is the volume of solution,  $M$  (g) is the mass of adsorbent.

During the adsorption procedure, we investigated the influences of the initial Pb<sup>2+</sup> concentration, pH of solution and contact time on the adsorption of series GO. Meanwhile, the adsorption isotherms were used to ascertain the adsorption process.

## Results and Discussion

### Characterization of series GO

#### FT-IR

Figure 1 shows the FT-IR spectra of graphite and series GO. In the spectra of graphite, the stretching vibrations peak of C=C could be found at 1628 cm<sup>-1</sup>, which also appeared in the other four spectra. Compared to the spectra of graphite, some characteristic peaks of oxygen-containing groups appeared in the spectra of series GO obviously. The adsorption peak appeared at 1072 and 1229 cm<sup>-1</sup> belonged to the stretching vibration of epoxy groups (C-O) and alkoxy groups (C-O) respectively. The adsorption peak appeared at 1390 and 1726 cm<sup>-1</sup> should be ascribed to the asymmetric and symmetric stretching vibrations of  $\nu$ -COOH. However, compared with GO-2, GO-3 and GO-4, there was no peaks at 1726 cm<sup>-1</sup> in the spectra of GO-1, which indicated that the GO-1 has been oxidized incompletely. In

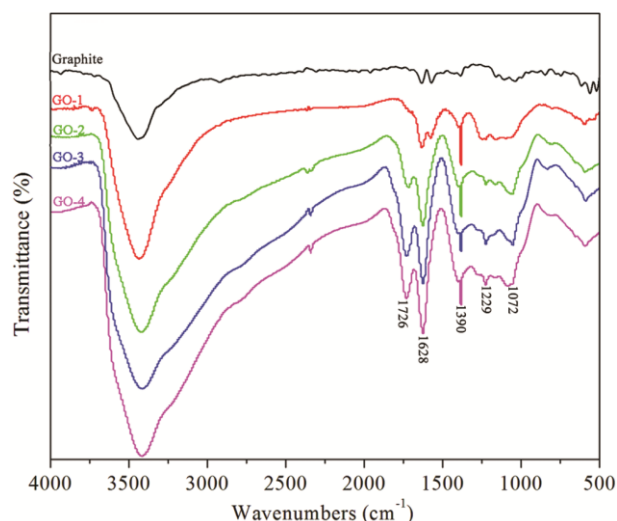


Fig. 1 — FT-IR spectra of graphite and series GO (GO-1, GO-2, GO-3, GO-4)

summary, we have prepared four kinds of oxidation grapheme successfully, meanwhile, the four kinds of GO showed different oxidation degree.

As shown in Fig. 2, the typical sharp diffraction peak of graphite could be found at  $2\theta=25.6$  in the graphite pattern. For GO-1, two diffraction peaks appear at  $2\theta=25.6$  and  $2\theta=12.2$  simultaneously, indicating that the graphite has been oxidized partly. For GO-2, GO-3 and GO-4, the typical sharp diffraction peak of graphite has disappeared and the diffraction peak of graphite oxide appeared at  $2\theta=11.6$ ,  $2\theta=11.1$  and  $2\theta=11.2$  respectively, which means that these three kinds of GO have been oxidation completely. In addition, the interlayer spacing of series GO increased with the increasing amount of oxidant (K<sub>2</sub>MnO<sub>4</sub>), and the layer spacing between GO-3 and GO-4 is relatively close<sup>3</sup>.

#### Morphology analysis

The morphologies of graphite and series GO have been characterized by TEM and SEM, as shown in Fig. 3 and Fig. 4. It is obvious that the lamellar thickness of series GO are thinner than that of graphite, which indicated that the structure of graphite changed from compact stacked multilayer structure to few or monolayer structure after oxidation. And the lamellar thickness of series GO decreased with the increasing amount of oxidant (K<sub>2</sub>MnO<sub>4</sub>). These results were probably caused by the intercalation of oxygen-containing functional groups in the interlayer space and consequent expansion of GO layers along the z-axis<sup>17</sup>. Anyway, the results obtained from TEM and SEM are assistant with the results given by FT-IR and XRD.

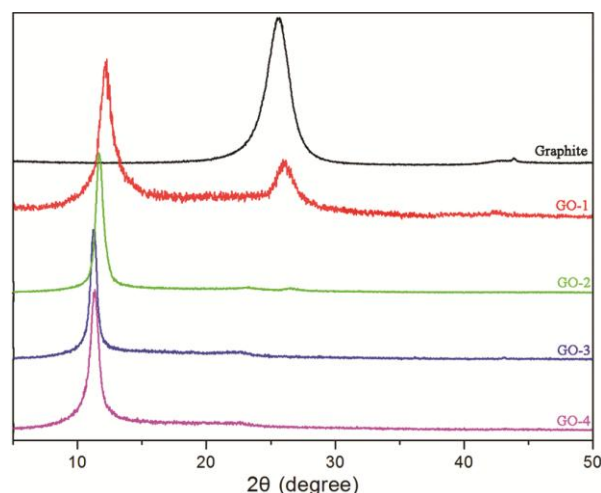


Fig. 2 — XRD patterns of graphite and series GO (GO-1, GO-2, GO-3, GO-4)

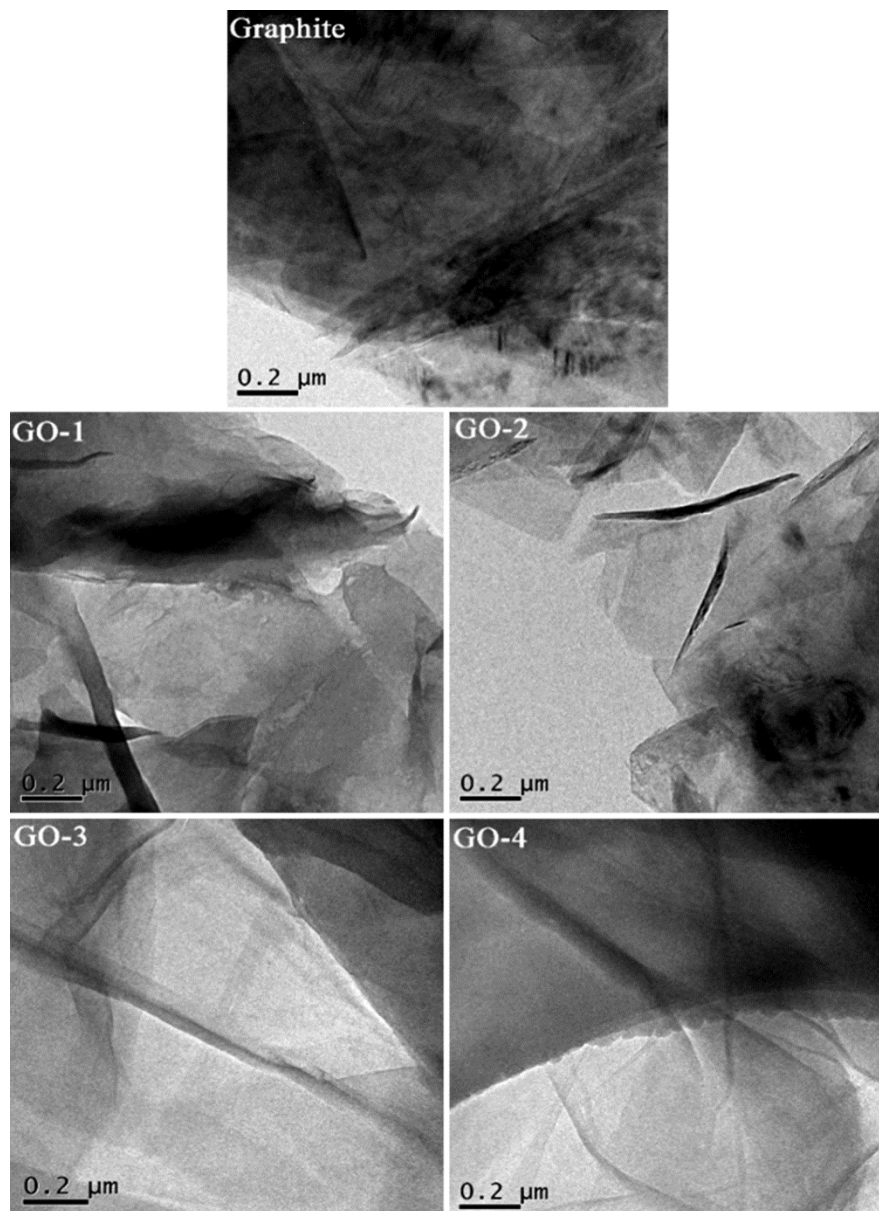


Fig. 3 — TEM images of graphite and series GO (GO-1, GO-2, GO-3, GO-4)

#### EDS

The element composition of graphite and series GO have been examined by EDS, and the results were showed in Table 2. For graphite, there was no oxygen element but all carbon element. After oxidation, oxygen element could be detected in GO-1, GO-2, GO-3 and GO-4. The amount of oxygen element increased obviously from GO-1 to GO-4, while the amount of carbon element decreased at the same time, as shown in Fig. 5. This result also proved that we have prepared series GO with different oxidation degree successfully and the oxidation degree increased with the increasing amount of  $\text{KM}_n\text{O}_4$  obviously.

#### Zeta-potential

The zeta-potential of series GO have been detected and shown in Table 3. For any kind of GO, the zeta-potential became more negative with the increasing of  $p\text{H}$  value. Meanwhile, the zeta-potential also became more negative with increasing of the oxidation degree of GO at the same  $p\text{H}$ , even the zeta-potential of GO-1 is positive (33.5 mV) at  $p\text{H}=2$ . It is attributed to that a mass of oxygen containing groups (-OH, -COOH) with negative charges have been introduced to the surface or edge of GO after oxidation, and these groups could be ionized to make GO more negative when  $p\text{H}$  increased<sup>17</sup>. Thus, the

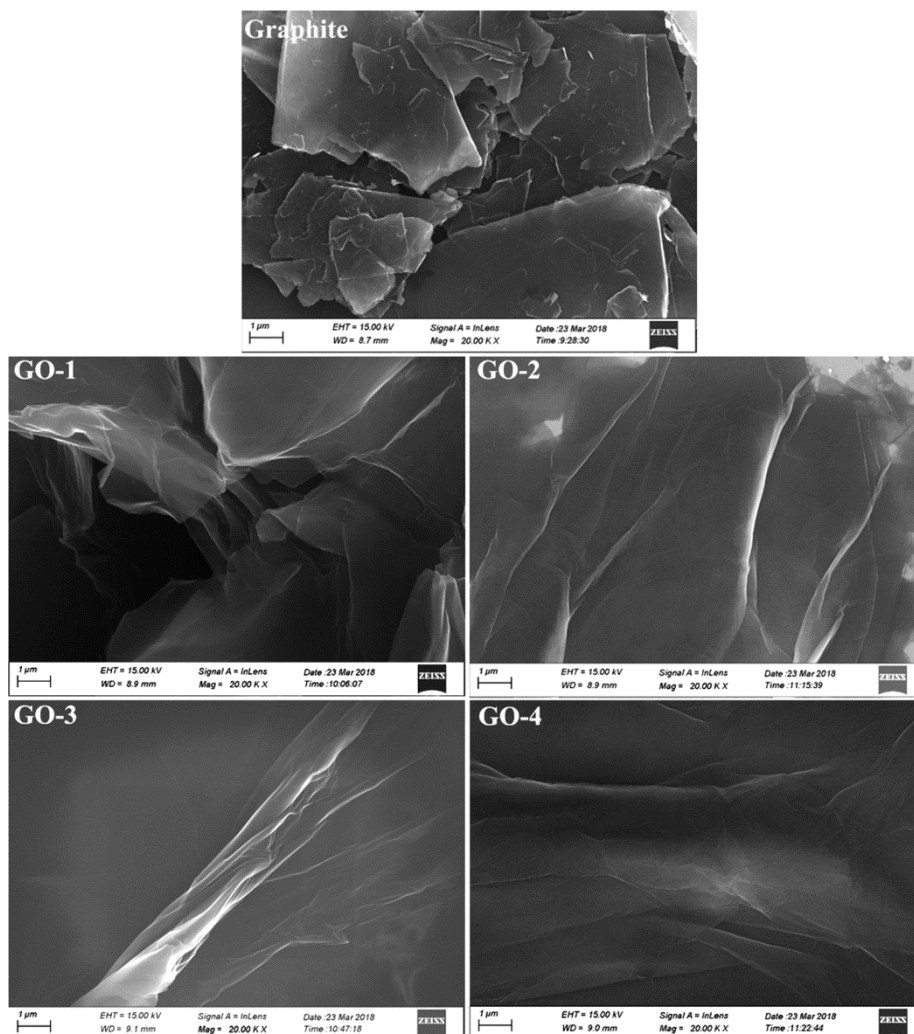


Fig. 4 — SEM images of graphite and series GO (GO-1, GO-2, GO-3 and GO-4)

Table 2 — The element composition of graphite and series GO

Samples	Graphite	GO-1	GO-2	GO-3	GO-4
wt%(C)	100	72.41	65.52	51.29	40.01
wt%(O)	0	27.59	34.48	48.71	59.99

zeta-potential also influenced by the oxidation degree of GO obviously.

### Adsorption

#### *Effect of initial $Pb^{2+}$ concentration*

The effect of initial concentration (100, 200, 300, 400, 500, 600 mg/L) on the adsorption capacity of series GO for  $Pb^{2+}$  has been carried out and shown in Fig. 6. With the increasing initial  $Pb^{2+}$  concentration, all of the adsorption quality ( $Q_e$ ) of series GO increased, while the removal efficiency (R%) decreased. For series GO with different oxidation degree, GO-3 displayed the best adsorption capacity,

for which, R% reached 92.5%, and GO-1 displayed a lowest adsorption capacity (R%=77.0%). In addition, GO-2 also showed a good adsorption capacity with R% of 86.7%. The adsorption capacity of GO-4 is lower than both of GO-2 and GO-3, although GO-4 has the highest oxidation of degree. Theoretically, the adsorption capacity of GO should increase with the increasing oxidation degree<sup>17</sup>. Herein, the low capacity of GO-4 may be explained by two aspects: on one hand, the agglomeration of ultra-thin layers may decrease the specific surface area of GO-4 and the adsorption active site for binding  $Pb^{2+}$  would also be reduced; on the other hand, the high oxidation degree



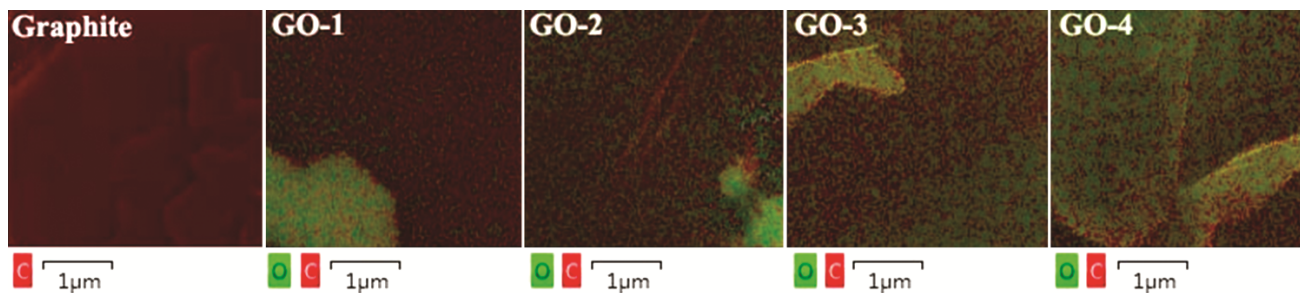


Fig. 5 — EDS images of graphite and series GO

Table 3 — Zeta-potential of series GO (mV)

pH	GO-1	GO-2	GO-3	GO-4
2	33.5	-27.3	-32.1	-35.9
3	-13.5	-32.7	-36.4	-38.6
4	-34.1	-33.1	-39.9	-39.8
5	-34.8	-36.7	-39.2	-45.4
6	-38.1	-42.1	-43.4	-45.7
7	-38.7	-43.4	-44.6	-46.6

of GO-4 not only enhance the electrostatic attraction and surface complexation, but also decrease the Lewis acid-base interaction between  $Pb^{2+}$  and aromatic groups of GO<sup>14,15</sup>. Thus, the order of adsorption capacity is: GO1<GO-4<GO-2<GO-3.

#### Effect of pH

The effects of pH ranging from 2.0 to 6.0 on the adsorption of series GO for  $Pb^{2+}$  were investigated and the results are given in Fig. 7. As the pH increased, the adsorption capacities of the series GO increased obviously, and the increasing trend of adsorption capacity tends to gentle after pH value above 4.0, which means that the  $Pb^{2+}$  adsorption on GO is effected strongly by solution pH. According to the results of zeta potential given in table 2, all of the series GO displayed negative charge under test conditions (except GO-1 at pH=2) and the zeta-potential became more negative with the increasing pH, thus, the electrostatic attraction between GO and  $Pb^{2+}$  also would be enhanced with increasing pH. At low pH levels, the existence of large number of  $H^+$  and  $H_3O^+$  in the solution may compete with  $Pb^{2+}$  for adsorption<sup>18</sup>, when the pH level increases, the covered  $H_3O^+$  leave the GO surface and made the sites available to  $Pb^{2+}$ , and the GO allowed more ligands to form complexes with  $Pb^{2+}$ . As a result, it is improved that the main adsorption mechanism of GO for  $Pb^{2+}$  are electrostatic attraction and complexation reaction<sup>13</sup>. Additionally, the order of adsorption capacity in this test is consistent with that in the test of 3.2.1: GO1<GO-4<GO-2<GO-3.

#### Effect of contact time

The effect of contact time (2, 4, 6, 8, 10 and 12 h) on the adsorption of series GO for  $Pb^{2+}$  was studied. As shown in Fig. 8, the adsorption capacity of series GO increased obviously within 6 h, and the adsorption reached to equilibrium after 6 h. Generally, the kinetics of heavy metal ions adsorption follow a two-stage process<sup>1</sup>. In the beginning of the adsorption process, large active sites are available for the sorbate and the process proceeds very fast. However, as the active sites are filled up, the adsorption proceeds slowly until the equilibrium is reached<sup>4</sup>.

#### Adsorption isotherms

Adsorption isotherm models are commonly used to describe the adsorption and its mechanisms. Herein, Langmuir, Freundlich, Temkin and Dubinin-Radushkevich isotherm models were applied to analyze the adsorption process for  $Pb^{2+}$  uptake at different concentrations.

The Langmuir isotherm model is often applied to homogeneous monolayer adsorption assuming that the affinity of adsorption sites on the adsorbent to adsorbate is equal. Langmuir isotherm is expressed as follow<sup>19</sup>:

$$\frac{C_e}{Q_e} = \frac{1}{K_L Q_m} + \frac{C_e}{Q_m} \quad \dots (1)$$

$$R_L = \frac{1}{1 + K_L C_o} \quad \dots (2)$$

where  $Q_e$  (mg/g) is the amount of  $Pb^{2+}$  adsorbed at equilibrium concentration,  $Q_m$  (mg/g) is the maximum adsorption amount during the adsorption process,  $C_e$

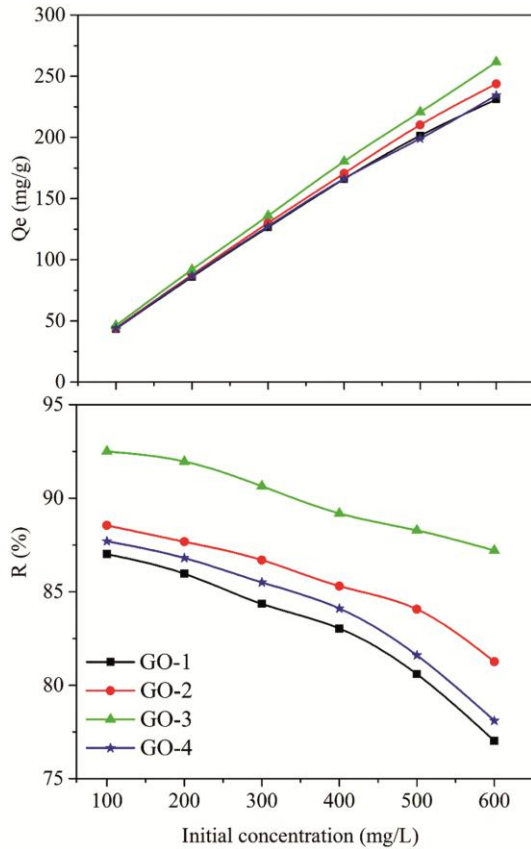


Fig. 6 — Effect of initial concentration on the adsorption of Pb<sup>2+</sup> on GO-1, GO-2, GO-3 and GO-4 (0.1g adsorbent, pH=6.0, T=25 °C, contact time=12 h)

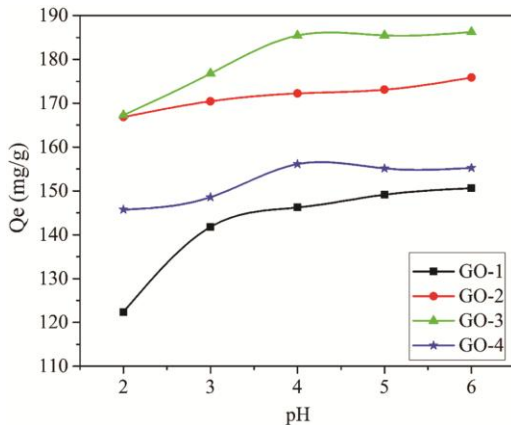


Fig. 7 — Effect of pH on the adsorption of Pb<sup>2+</sup> on GO-1, GO-2, GO-3 and GO-4 (0.1g adsorbent, initial Pb<sup>2+</sup> concentration=400 mg/L, T=25 °C, contact time=12h)

(mg/L) is the concentration of Pb<sup>2+</sup> in the solution at equilibrium,  $K_L$  (L/mg) is the Langmuir binding constant related to the energy of adsorption. The value of  $R_L$  reveals the type of isotherm to be favorable ( $0 < R_L < 1$ ), unfavourable ( $R_L > 1$ ), linear ( $R_L = 1$ ), or irreversible ( $R_L = 0$ )<sup>20</sup>.

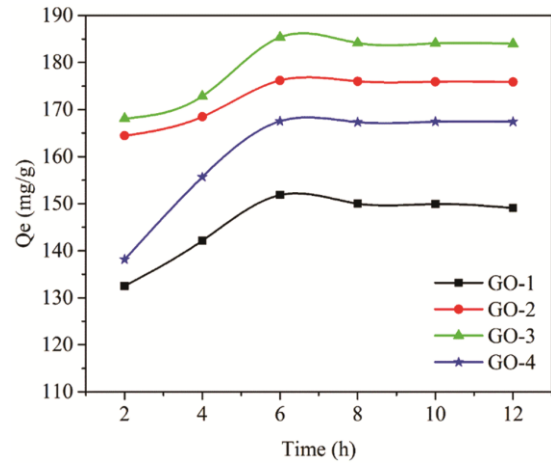


Fig. 8 — Effect of contact time on the adsorption of Pb<sup>2+</sup> on GO-1, GO-2, GO-3 and GO-4 (0.1g adsorbent, initial Pb<sup>2+</sup> concentration =400 mg/L, pH=4, contact time=12h)

The Freundlich isotherm is derived by assuming a heterogeneous surface with a nonuniform distribution of the heat of sorption over the surface. It can be linearly expressed as follows<sup>19</sup>:

$$\ln Q_e = \ln K_F + \frac{1}{n} \ln C_e \quad \dots(3)$$

where  $K_F$  and  $1/n$  are the Freundlich constants, indicating the adsorption capacity and adsorption intensity, respectively. If the value of  $1/n$  is lower than 1, it indicates a normal Langmuir isotherm; otherwise, it is indicative of cooperative adsorption<sup>5</sup>.

Temkin and Pyzhev considered the effects of some indirect adsorbent–adsorbate interaction on adsorption isotherms and suggested that the heat of adsorption of all the molecules in the layer would linearly decrease with coverage because of these interactions<sup>5</sup>. The Temkin isotherm has been applied in the following form:

$$Q_e = B_T \ln A_T + B_T \ln C_e \quad \dots(4)$$

$$B_T = \frac{RT}{b_T} \quad \dots(5)$$

where  $R$  is gas constant (8.314 J/(mol.K)),  $T$  (K) is the temperature,  $b_T$  (J/mol) is related to the heat of adsorption,  $A_T$  (L/g) is equilibrium binding constant.

The Dubinin–Radushkevich (D-R) isotherm model assumed that the mechanism for adsorption in micropores is that of pore-filling rather than layer-by-layer surface coverage. It is generally utilized to calculate the adsorption energy, which can predict the nature of adsorption process i.e. physical or chemical<sup>21</sup>. D-R isotherm is expressed as follow:

$$\ln Q_e = \ln Q_m - \beta \varepsilon^2. \quad \dots (6)$$

$$\varepsilon = RT \ln \left( 1 + \frac{1}{C_e} \right) \quad \dots (7)$$

$$E = \frac{1}{\sqrt{2\beta}} \quad \dots (8)$$

where  $\varepsilon^2$  (kJ/mol) is the Polanyi potential calculated using Eq. (6),  $\beta$  (mol<sup>2</sup>/kJ<sup>2</sup>) is the activity coefficient related to mean adsorption energy,  $E$  (kJ/mol) is defined as the mean free energy and used to estimate the type of adsorption reaction.

The four different adsorption isotherms were obtained by using linear fitting at different initial concentration as shown in Fig. 9, and the relevant parameters are presented in Table 4. The adsorption of Pb<sup>2+</sup> adsorbed on series GO are fitted to the Langmuir isotherm model with the highest R<sup>2</sup>, which implied that the adsorption process was homogeneous monolayer coverage. Additionally, the maximum adsorption capacity calculated by Langmuir isotherm is closed to the experimental results. Furthermore, the value of  $n$  in the Temkin isotherm model is greater than 1, thus the adsorption process was considered favorable<sup>22,23</sup>.

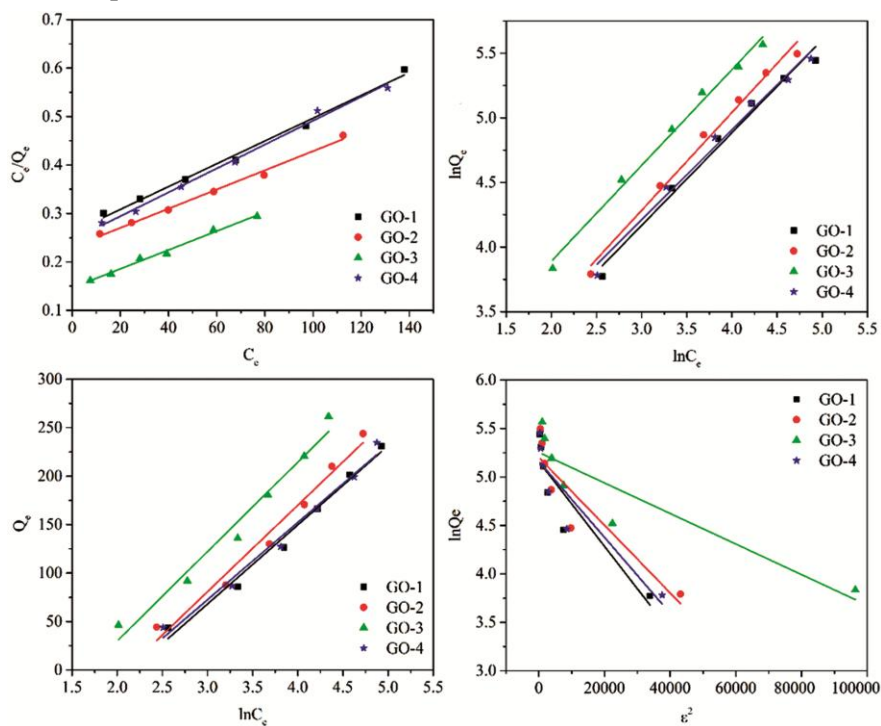


Fig. 9 — The adsorption isotherm model of Pb<sup>2+</sup> adsorption on series GO: a. Langmuir model, b. Freundlich model, c. Temkin model, d. Dubinin–Radushkevich model

Table 4 — Adsorption isotherm model constants of three isotherm models for Pb<sup>2+</sup> adsorption on series GO

Model	Constant	GO-1	GO-2	GO-3	GO-4
Langmuir	R <sup>2</sup>	0.9939	0.9931	0.9925	0.9933
	Q <sub>max</sub> (mg/g)	216.67	300.00	326.32	230.00
	K <sub>L</sub> (L/mg)	0.0178	0.0144	0.0209	0.0177
Freundlich	R <sup>2</sup>	0.9812	0.9873	0.9895	0.9831
	K <sub>F</sub> (mg/g)	7.5157	7.4663	11.1128	8.3187
	$n$	1.3947	1.3196	1.3492	1.4345
Temkin	R <sup>2</sup>	0.9846	0.9779	0.9732	0.9820
	A <sub>T</sub> (L/g)	0.1147	0.1231	0.1873	0.1235
	B <sub>T</sub> (J/mol)	81.596	89.239	92.246	79.769
D-R	R <sup>2</sup>	0.8406	0.8360	0.8343	0.8438
	Q <sub>m</sub> (mg/g)	188.76	217.29	229.37	273.25
	E (kJ/mol)	111.80	129.10	158.11	11.80



## Conclusion

In this study, four kinds of GO with different oxidation degree have been prepared successfully by a modified Hummers' method with variation of the amount of KM<sub>n</sub>O<sub>4</sub>. The series GO were used to adsorb Pb<sup>2+</sup> from waste water and they displayed different adsorption capacity: GO-3>GO-2>GO-4>GO-1. It means that the adsorption capacity does not always increase with the increase of oxidation degree, and the adsorption capacity may be reduced by the aggregation of GO sheet and the destroying of sp<sup>2</sup>-hybridized structure when the GO has higher oxidation degree. The adsorption process of series GO for Pb<sup>2+</sup> were well described by the Langmuir isotherm model, which revealed that the adsorption process was homogeneous monolayer coverage.

## Acknowledgements

The author thanks the financial supports from the Ningxia Higher Education Research Project (NGY2018-150), National Natural Science Foundation of Ningxia (2019AAC03116) and Key Scientific Research Project Foundation of North Minzu University (2019KJ09).

## References

- 1 Burakov A E, Galunin E V, Burakova I V, Kucherova A E, Agarwal S, Tkachev A G & Gupta V K, *Ecotoxicol Environ Saf*, 702 (2018) 148.
- 2 Demiral H & Güngör C, *J Clean Prod*, 103 (2016) 124.
- 3 Tan P, Hu Y & Bi Q, *Colloid Surface A*, 56 (2016) 509.
- 4 Zhao D, Gao X, Wu C, Xie R, Feng S & Chen C, *Appl Surf Sci*, 1 (2016) 384.
- 5 Mi X, Huang G, Xie W, Wang W, Liu Y & Gao J, *Carbon*, 4856 (2012) 50.
- 6 Gui C X, Wang Q Q, Hao S M, Qu J, Huang P P, Cao C Y, Song W G & Yu Z Z, *Appl Mater Inter*, 14653 (2014) 6.
- 7 Li X, Zhou H, Wu W, Wei S, Xu Y & Kuang Y, *J Colloid Interf Sci*, 389 (2015) 448.
- 8 Peng W, Liu Y & Song S, *J Mol Liq*, 496 (2017) 230.
- 9 Chen D, Zhang H, Yang K & Wang H, *J Hazard Mater*, 179 (2016) 310.
- 10 Liu S, Wang H, Chai L & Li M, *J Colloid Interf Sci*, 288 (2016) 478.
- 11 Zare Dorabei R, Ferdowsi S M, Barzin A & Tadjarodi A, *Ultrason Sonochem*, 265 (2016) 32.
- 12 Tadjarodi A, Moazen Ferdowsi S, Zare Dorabei R & Barzin A, *Ultrason Sonochem*, 118 (2016) 33.
- 13 Sherlala A I A, Raman A A A, Bello M M & Asghar A, *Chemosphere*, 1004 (2018) 193.
- 14 Motoi Machida T M & Tatsumoto H, *Carbon*, 2681 (2006) 44.
- 15 Huang Z H, Zheng X, Lv W, Wang M, Yang Q H & Kang F, *Langmuir*, 7558 (2011) 27.
- 16 Wang F, *Chem Eng Res Des*, 155 (2017) 128.
- 17 Tan P, Bi Q, Hu Y, Fang Z, Chen Y & Cheng J, *Appl Surf Sci*, 1141 (2017) 423.
- 18 Ma Y X, Xing D, Shao W J, Du X Y & La P Q, *J Colloid Interf Sci*, 352 (2017) 505.
- 19 Li Z, Qi M, Tu C, Wang W, Chen J & Wang A J, *Appl Surf Sci*, 765 (2017) 425.
- 20 Cheng J H, Xing H T, Sun X, Huang Y H, Su Z B, Hua S R, Weng W, Li S X, Guo H X, Wu W B, He Y S, Li F M & Huang Y, *Chem Eng J*, 280 (2015) 263.
- 21 Ahmad R & Haseeb S, *Desalin Water Treat*, 17826 (2016) 57.
- 22 Jay S, Nusrat S, Ayushi S & Shikha A, *J Mol Liquid*, 315 (2020) 113766.
- 23 Verma M, Tyagi I, Chandra R & Kumar V, *J Mol Liquid*, 225 (2017) 936.